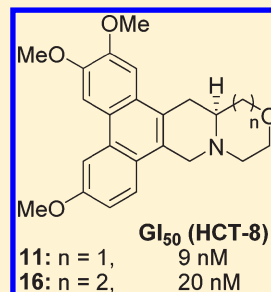


Antitumor Agents 288: Design, Synthesis, SAR, and Biological Studies of Novel Heteroatom-Incorporated Antofine and Cryptopleurine Analogues as Potent and Selective Antitumor Agents

Xiaoming Yang,[†] Qian Shi,^{*,†} Shuenn-Chen Yang,[§] Chi-Yuan Chen,[§] Sung-Liang Yu,^{||,▽} Kenneth F. Bastow,[‡] Susan L. Morris-Natschke,[†] Pei-Chi Wu,[‡] Chin-Yu Lai,[⊥] Tian-Shung Wu,[○] Shioh-Lin Pan,[⊥] Che-Ming Teng,[⊥] Jau-Chen Lin,[§] Pan-Chyr Yang,^{*,⊥,§,#} and Kuo-Hsiung Lee^{*,†,○}[†]Natural Products Research Laboratories and [‡]Division of Medicinal Chemistry and Natural Products, Eshelman School of Pharmacy, University of North Carolina, Chapel Hill, North Carolina 27599-7568, United States[§]Institute of Biomedical Sciences, Academia Sinica, Taipei, Taiwan^{||}Department of Clinical Laboratory Sciences and Medical Biotechnology, [⊥]Department of Internal Medicine, College of Medicine, and[#]Division of Genomic Medicine, Research Center for Medical Excellence, National Taiwan University, Taipei, Taiwan[▽]Department of Laboratory Medicine, National Taiwan University Hospital, Taipei, Taiwan[○]Chinese Medicine Research and Development Center, China Medical University and Hospital, Taichung 404, Taiwan

Supporting Information

ABSTRACT: Novel heteroatom-incorporated antofine and cryptopleurine analogues were designed, synthesized, and tested against a panel of five cancer cell lines. Two new S-13-oxo analogues (**11** and **16**) exhibited potent cell growth inhibition *in vitro* (GI₅₀: 9 nM and 20 nM). Interestingly, both compounds displayed improved selectivity among different cancer cell lines, in contrast to the natural products antofine and cryptopleurine. Mechanism of action (MOA) studies suggested that R-antofine promotes dysregulation of DNA replication during early S phase, while no similar effects were observed for **11** and **15** on corresponding replication initiation complexes. Compound **11** also showed greatly reduced cytotoxicity against normal cells and moderate antitumor activity against HT-29 human colorectal adenocarcinoma xenograft in mice without overt toxicity.



INTRODUCTION

Phenanthroindolizidines and phenanthroquinolizidines, which are natural alkaloids isolated from several plant species such as the *Asclepiadaceae* and *Moraceae* family,¹ have been investigated intensively in recent years, due to their interesting biological characteristics, including antimicrobial, antiangiogenic, and anti-inflammatory effects,^{2–8} as well as significant cytotoxicity as demonstrated in the NCI 60 cell-line assay (Figure 1).⁹ Further studies have shown that these natural products exhibit not only strong inhibitory activity against cancer cell growth but also significant effects on cancer cells resistant or cross-resistant to many anticancer drugs in the market.¹⁰ Thus, this important class of chemical entities may potentially augment our present arsenal of anticancer drugs.^{11,12}

Although the biological target(s) and MOA of these natural products are currently still unclear, some interesting findings have been reported. A possible mechanism of action might be inhibition of NF- κ B signaling, a well-known pathway in the antiapoptosis and survival of cancer cells, as well as regulation of P-glycoprotein.¹³ Other hypotheses, such as inhibition of protein synthesis during the chain elongation stage,¹⁴ targeting ribosomal subunits (low-affinity binding pockets have been identified in the 40S, 60S, 70S, and 80S subunits),^{15–17} inhibition of

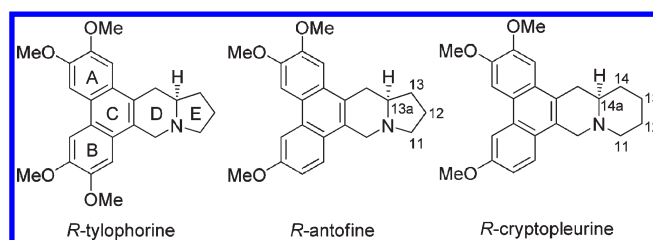
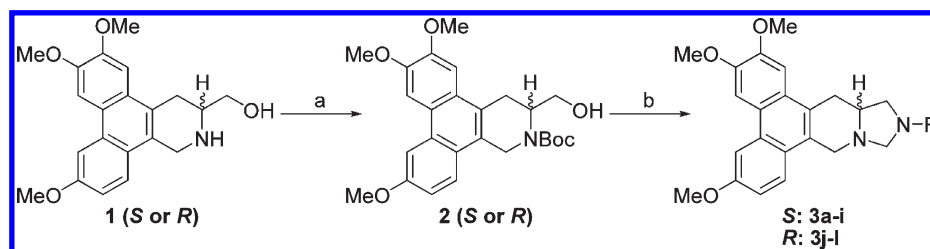


Figure 1. Representative structures of phenanthroindolizidines and phenanthroquinolizidines.

hypoxia-inducible factor 1 (HIF-1),¹⁸ inhibition of thymidylate synthase (TS) and dihydrofolate reductase (DHFR),^{19–21} suppression of activator protein-1 (AP-1) and the cAMP response element (CRE) signaling pathway, reduction of cell cycle regulatory proteins such as cyclin D₁, cyclin B₁, CDK₁, CDK₂, and CDK₄, etc.¹⁰ have also been reported. In addition, evidence has suggested that certain structural analogues might not be functional analogues,²² and thus, multiple biological targets might exist.

Received: March 22, 2011

Published: June 13, 2011

Scheme 1^a

^a Reagents and conditions: (a) (Boc)₂O, Et₃N, CH₂Cl₂; (b) (i) Py·SO₃, DMSO, Et₃N, CH₂Cl₂; (ii) RNH₂, HOAc, NaBH₃CN, MeOH; (iii) TFA, CH₂Cl₂; (iv) K₂CO₃, MgSO₄, HCHO, CH₂Cl₂.

Despite their promise, the potential development of antofine, cryptopleurine, or related natural or synthetic alkaloids as promising drug candidates has been limited, to a large degree, by severe CNS toxicity, such as disorientation and ataxia,²³ and low natural availability. All of these factors combine to justify an urgent need for improving the pharmacokinetic and pharmacodynamic properties, such as polarity, of this compound class through rational structural modifications. However, only limited studies have been reported in this regard, e.g., introduction of a hydroxy group at C14 of phenanthroindolizidines,²⁴ construction of phenanthrene-based tylophorine analogues,^{25–27} and N atom incorporation at C13a of tylophorine,²⁸ probably due to the lack of a convergent and efficient synthetic methodology. Recently, our group reported a new strategy suitable for producing numerous new phenanthroindolizidine and phenanthroquinolizidine analogues with E-ring modifications.²⁹ The versatility and significance of this approach lie in the fact that it not only facilitates the SAR study of E-ring variations but also, even more importantly, generates a group of analogues carrying a heterocyclic E-ring or other polar moieties to potentially overcome CNS toxicity. CNS toxicity is closely associated with the blood–brain barrier (BBB) penetration of a molecule, which is in large part related to its physicochemical properties, such as lipophilicity (cLogP) or polarity, molecular size and charge, polar surface area (PSA), or hydrogen bonding potential, etc., although other factors may also play a role.^{30–32} Herein, we report the design, synthesis, *in vitro* anticancer activity, SAR, and mechanistic studies of new antofine and cryptopleurine derivatives with a N or O atom incorporated in the E-ring. The *in vivo* antitumor activity for the most active compound (**11**) is also reported.

RESULTS AND DISCUSSION

Initially, antofine analogues bearing a N atom at position C12 were designed and synthesized. The key intermediate **1** was prepared via a procedure recently reported by our group.²⁷ The amino group of **1** (S or R isomer) was protected initially with a Boc group to give **2**. Then the hydroxy group was oxidized with Py·SO₃ to an aldehyde, which was then converted to various secondary amines through reductive amination using NaBH₃CN. After the removal of the Boc group, **3a–3l** were obtained through cyclization with formaldehyde (Scheme 1).

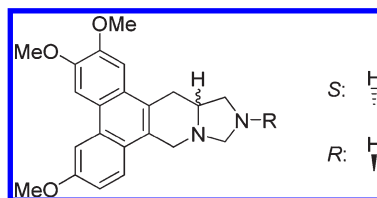
Compounds **3a–3l** were then screened against four cancer cell lines, A549 (lung), DU-145 (prostate), KB (nasopharyngeal), and HCT-8 (colon). The screening results are shown in Table 1. In comparison with *R*-antofine, all 12 compounds exhibited substantially decreased activity with an average GI₅₀ over 1 μM. In addition, no cell-line selectivity was observed. Compound **3f** (R = Ph) was the least potent (inactive) with an average GI₅₀ value

greater than 20 μM. Insertion of a single methylene group between the N and phenyl ring (**3a** and **3j**, R = CH₂Ph) resulted in greater activity (with the *R* isomer approximately 2-fold better than the *S* isomer), while addition of a second methylene group (**3d**, R = CH₂CH₂Ph) did not improve activity any further. Generally, the compounds with an aliphatic amino moiety [cyclic (**3g**), straight chain (**3c**, **3h**, and **3l**), or branched chain (**3b**)] showed slightly better activity than those bearing an aromatic moiety. Compounds **3h** and **3l** (R = Me) showed the greatest potency among all compounds, and the *R* isomer (**3l**) was slightly more potent than its *S* enantiomer (**3h**). Conversely, **3i** (*S* isomer) was 2-fold more active than its *R* isomer (**3k**). These data implied that introduction of a N atom at position C12 of antofine might not improve the cytotoxicity against cancer cell lines, even though it did increase the polarity as predicted by PreADMET.³³

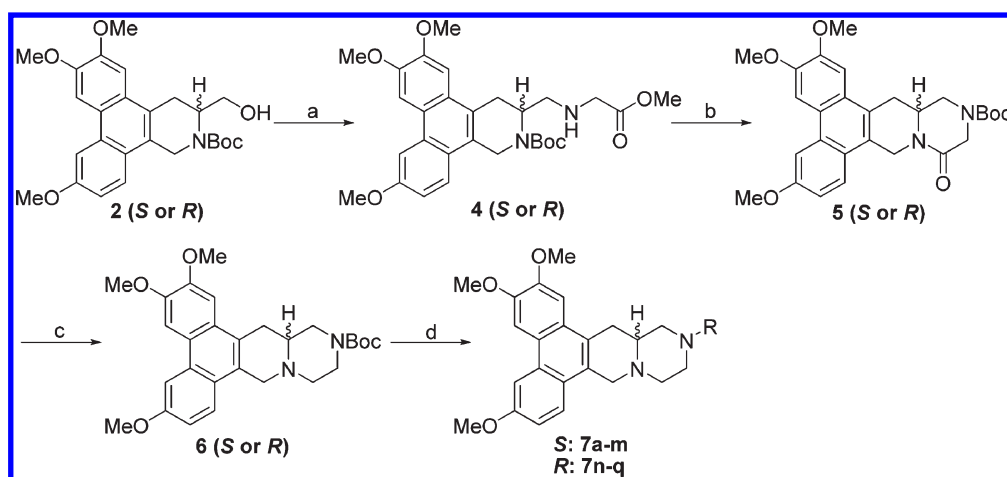
Next, we studied the effect of N-incorporation in cryptopleurine, both at positions C12 and C13. For the latter compound series, **2** (S or R) was converted to **4** through oxidation with Py·SO₃ and subsequent reductive amination using glycine methyl ester hydrochloride. The E ring was formed by sequential deprotection with HCl/MeOH and cyclization with Et₃N/MeOH. The resulting intermediate was further protected with a Boc group to give **5** for easy purification. The lactam carbonyl was then reduced to a methylene using BMS/THF to afford **6**. After the removal of the Boc group, 13-aza-cryptopleurines (**7a–q**) were obtained through either acylation or reductive amination (Scheme 2).

The GI₅₀ values of **7a–q** are listed in Table 2. Although the 13-aza analogues showed significantly reduced activity as compared with that of *R*-cryptopleurine, some interesting results were observed. Compound **7g**, with a *N*-cyclopropylmethyl substituent, was the most potent analogue against the HCT-8 cell line with a GI₅₀ value of 0.25 μM, in addition to better selectivity against A549 and HCT-8 versus DU145 and KB. However, **7h**, with a *N*-cyclopropyl substituent, one –CH₂– shorter than **7g**, showed dramatically reduced activity. Similar results were observed from the comparison of **7c** and **7f**, as well as antofine analogues **3f**, **3a**, and **3d**, suggesting that the length of the side chain on nitrogen affects the anticancer activity. It is also interesting to note that **7g** was much more potent than its *R* isomer **7q**, whereas **7m** and **7p** exhibited the reversed order of activity, although to a less significant degree. Of all the tested analogues in this series, compound **7a**, the hydrochloride salt of 13-aza-cryptopleurine, showed considerable anticancer activity against all four tested cell lines, indicating that **7a** might be a promising lead meriting further investigation.

In the following studies, a series of cryptopleurine analogues (**10a–j**) with N replacement at position C12 were synthesized to

Table 1. GI₅₀ Values of 12-Aza-antofines 3a–l against Four Cancer Cell Lines

compd.	R	Config.	AS49 (μM)	DU145 (μM)	KB (μM)	HCT-8 (μM)
3a	-Bn	S	5.30 \pm 1.02	4.95 \pm 1.24	5.70 \pm 1.52	3.63 \pm 0.81
3b	-iBu	S	2.00 \pm 0.36	6.60 \pm 1.45	4.40 \pm 1.23	1.82 \pm 0.45
3c	-nPr	S	3.94 \pm 0.78	7.38 \pm 1.55	6.64 \pm 1.73	2.71 \pm 0.49
3d	-(CH ₂) ₂ Ph	S	6.62 \pm 2.04	10.20 \pm 3.13	10.03 \pm 2.11	7.47 \pm 1.68
3e	-2'-OH-Et	S	4.41 \pm 0.97	6.36 \pm 1.29	7.83 \pm 1.59	10.77 \pm 2.44
3f	-Ph	S	>20	>20	>20	>20
3g	-cPr	S	1.80 \pm 0.36	3.70 \pm 0.81	2.71 \pm 0.89	1.85 \pm 0.48
3h	-Me	S	0.66 \pm 0.11	2.03 \pm 0.38	1.72 \pm 0.55	1.00 \pm 0.19
3i	-NMe ₂	S	1.67 \pm 0.37	2.26 \pm 0.47	2.31 \pm 0.65	2.01 \pm 0.54
3j	-Bn	R	2.68 \pm 0.51	4.62 \pm 1.16	3.41 \pm 0.78	1.87 \pm 0.43 (KBvin)
3k	-NMe ₂	R	4.15 \pm 0.87	6.01 \pm 1.50	2.38 \pm 0.60	10.98 \pm 2.92 (KBvin)
3l	-Me	R	0.66 \pm 0.10	1.00 \pm 0.23	0.79 \pm 0.21	0.66 \pm 0.16
R-antofine		R	22 \pm 7 nM	25 \pm 5 nM	36 \pm 8 nM	-

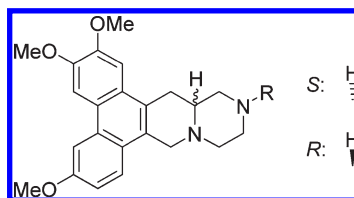
Scheme 2^a

^a Reagents and conditions: (a) (i) Py·SO₃, DMSO, Et₃N, CH₂Cl₂; (ii) glycine methyl ester hydrochloride, Et₃N, HOAc, NaBH₃CN, MeOH; (b) (i) HCl, MeOH; (ii) MeOH, Et₃N; (iii) (Boc)₂O, Et₃N, CH₂Cl₂; (c) BMS, THF; (d) (i) TFA, CH₂Cl₂; (ii) RCOCl, Et₃N, CH₂Cl₂ or RCHO, Et₃N, HOAc, NaBH₃CN, MeOH.

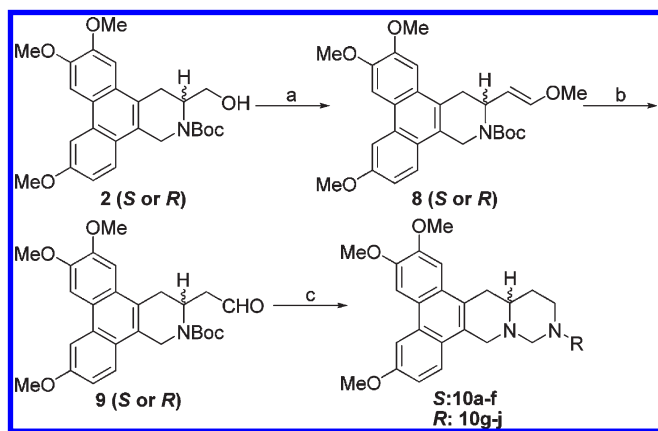
explore their anticancer activity. Compound **2** was converted to vinylmethyl ether **8** in two steps, oxidation followed by a Wittig reaction using Ph₃P=CH₂OMe. Compound **8** was then hydrolyzed with Hg(OAc)₂ to give aldehyde **9**. The targets, 12-aza-cryptopleurines **10a–j**, were prepared using a strategy similar to that described in the synthesis of compounds **3a–l** (Scheme 3).

The GI₅₀ values for **10a–j** are listed in Table 3. Overall, the results suggested that N-incorporation at position C12 of cryptopleurine diminished the anticancer activity (lowest GI₅₀ value was 1.12 μM for a 12-aza analogue **10j** versus nM values for cryptopleurine). Anticancer activity patterns similar to those described above with the other compound series were observed.

Compounds with bulky or aromatic groups, such as a phenyl or benzyl moiety (**10b** or **10d**), exhibited lower activity (>20 μM), as also observed in the above two series of analogues. Introducing a polar group, such as hydroxyethyl in **10a/10i** and N,N-dimethylamino in **10f/10h**, did not lead to increased activity, although some moderate cell-line selectivity was found. The stereochemistry of the analogues also affected the anticancer activity (compare **10a/10i**, **10c/10g**, and **10f/10h**), as was also observed in the above two analogue series, although the trends were neither significant nor consistent. Interestingly, in the comparison of **10j** and **7q** (N12 vs N13 substitution), the former compound was significantly more potent than the latter.

Table 2. GI₅₀ Values of 13-Aza-cryptopleurines 7a–q against Four Cancer Cell Lines

compd.	R	config.	A549 (μM)	DU145 (μM)	KB (μM)	HCT-8 (μM)
7a	H, HCl salt	S	1.73 \pm 0.52	2.08 \pm 0.27	1.79 \pm 0.37	1.62 \pm 0.56
7b	-Et	S	7.13 \pm 3.86	10.48 \pm 2.51	8.24 \pm 1.89	9.45 \pm 3.21
7c	-CO ₂ Me	S	10.93 \pm 5.10	12.19 \pm 3.04	11.32 \pm 2.25	12.05 \pm 2.58
7d	-Ac	S	11.65 \pm 1.88	11.94 \pm 2.22	15.46 \pm 2.78	13.82 \pm 2.80
7e	-Ms	S	14.52 \pm 3.02	16.97 \pm 3.14	17.52 \pm 3.10	17.83 \pm 3.63
7f	-CH ₂ CO ₂ Me	S	14.74 \pm 2.49	>20	14.65 \pm 2.88	14.03 \pm 2.12
7g	-CH ₂ cPr	S	0.79 \pm 0.11	2.94 \pm 0.45	6.57 \pm 1.56	0.25 \pm 0.11
7h	-cPr	S	>20	17.92 \pm 5.28	>20	13.02 \pm 3.03
7i	-Bz	S	15.00 \pm 3.77	15.71 \pm 4.32	>20	18.11 \pm 4.91
7j	-2'-OH-Et	S	14.08 \pm 5.49	12.62 \pm 5.61	8.62 \pm 2.44	7.41 \pm 1.30
7k	-PO(OMe) ₂	S	12.18 \pm 3.18	14.66 \pm 4.59	8.09 \pm 1.02	10.42 \pm 2.21 (KBvin)
7l	-Me	S	9.73 \pm 1.81	7.13 \pm 1.05	5.30 \pm 0.46	6.45 \pm 1.03
7m	-Bn	S	>20	>20	16.85 \pm 5.64	15.24 \pm 3.35 (KBvin)
7n	-CONMe ₂	R	14.08 \pm 1.86	13.12 \pm 1.98	12.32 \pm 2.15	11.41 \pm 2.10 (KBvin)
7o	-iBu	R	12.86 \pm 2.31	12.24 \pm 4.04	11.25 \pm 2.36	9.96 \pm 1.89 (KBvin)
7p	-Bz	R	16.43 \pm 6.08	11.87 \pm 3.92	12.14 \pm 2.91	7.64 \pm 1.07 (KBvin)
7q	-CH ₂ cPr	R	>20	>20	>20	13.44 \pm 2.42 (KBvin)
crypto-pleurine		R	1.38 \pm 0.56 nM	1.59 \pm 0.53 nM	1.51 \pm 0.33 nM	1.09 \pm 0.20 nM

Scheme 3^a

^a Reagents and conditions: (a) (i) Py·SO₃, DMSO, Et₃N, CH₂Cl₂; (ii) Ph₃P⁺CH₂OMeCl⁻, THF, KOtBu; (b) Hg(OAc)₂, THF, H₂O; (c) (i) RNH₂, HOAc, NaBH₃CN, MeOH; (ii) TFA, CH₂Cl₂; (iii) K₂CO₃, MgSO₄, HCHO, CH₂Cl₂.

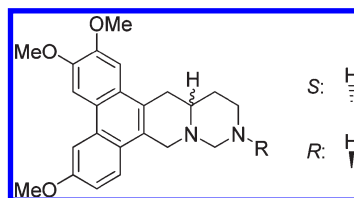
Likewise, **10g** was more potent than **7o**, likely indicating that the relocation of the N atom could cause a possible conformational change, which led to a differentiation in biological activity.

Even though the above modifications of antofine and cryptopleurine by N incorporation in the E-ring did not provide analogues with enhanced or at least comparable anticancer activity to the natural alkaloids, we extended our studies by

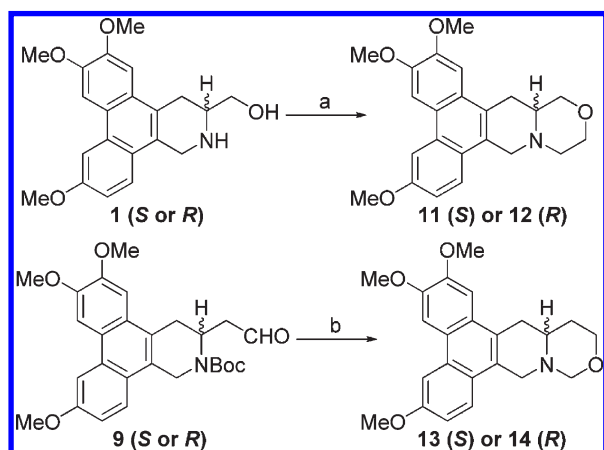
investigating the effect of O atom incorporation at corresponding positions. Unfortunately, introduction of the oxygen atom at position C12 of antofine was not successful due to the instability of the resulting analogue. However, incorporation of the O atom into the E-ring of cryptopleurine at position C12 or C13 was achieved, as described in Scheme 4.

Reaction of **1** with chloroacetyl chloride furnished the intermediate amide, which underwent intramolecular nucleophilic attack using NaH/THF and subsequent reduction using BMS/THF to afford *S*-13-oxo-cryptopleurine **11** and its *R* isomer **12**. For the O replacement at position C12 of cryptopleurine, the aldehyde of **9** was first converted to a hydroxymethyl group by NaBH₄ reduction, followed by removal of Boc and subsequent cyclization using HCHO to give *S*-12-oxo-cryptopleurine **13** and its *R* isomer **14** (Scheme 4).

A cytotoxicity evaluation of **11**–**14** against four cancer cell lines was conducted, and the results are summarized in Table 4. It is exciting to note that **11**, with O at position C13, exhibited potent nanomolar anticancer activity with greater selectivity toward the HCT-8 tumor cell line (GI₅₀ = 9 nM). In contrast, compound **12**, the *R*-enantiomer of **11**, showed significantly decreased activity. As for the incorporation of O at position C12, both analogues **13** and **14** exhibited much lower potency than *R*-cryptopleurine with GI₅₀ > 1 μM . The slight structural variation among **11**–**14** resulted in significantly different biological activity. Compound **11** might achieve a specific structural conformation that is required for interacting with the target protein leading to the observed anticancer activity. However, further studies are

Table 3. GI₅₀ Values of Analogues 10a–j against Four Cancer Cell Lines

compd.	R	config.	A549 (μM)	DU145 (μM)	KB (μM)	HCT-8 (μM)
10a	-2'-OH-Et	S	5.68 \pm 1.36	1.99 \pm 0.52	1.59 \pm 0.36	10.65 \pm 3.73
10b	-Ph	S	>20	>20	>20	>20
10c	-iBu	S	1.52 \pm 0.38	2.30 \pm 0.55	5.06 \pm 1.82	1.36 \pm 0.29
10d	-Bn	S	>20	>20	>20	>20
10e	-cPr	S	4.30 \pm 0.77	14.33 \pm 3.80	11.47 \pm 3.72	5.73 \pm 1.14
10f	-NMe ₂	S	1.78 \pm 0.43	2.97 \pm 0.51	3.08 \pm 0.50	2.37 \pm 0.78
10g	-iBu	R	5.11 \pm 1.62	1.66 \pm 0.43	1.45 \pm 0.22	7.32 \pm 1.90 (KBvin)
10h	-NMe ₂	R	5.20 \pm 1.02	3.00 \pm 0.65	2.84 \pm 0.56	5.30 \pm 1.18 (KBvin)
10i	-2'-OH-Et	R	2.48 \pm 0.36	1.46 \pm 0.33	2.22 \pm 0.41	>20 (KBvin)
10j	-CH ₂ cPr	R	1.12 \pm 0.29	1.20 \pm 0.28	2.10 \pm 0.39	5.68 \pm 1.53 (KBvin)
crypto-pleurine		R	1.38 \pm 0.56 nM	1.59 \pm 0.53 nM	1.51 \pm 0.33 nM	1.09 \pm 0.20 nM

Scheme 4^a

^a Reagents and conditions: (a) (i) ClCH₂COCl, Et₃N, CH₂Cl₂; (ii) NaH, THF, reflux; (iii) BMS, THF; (b) (i) NaBH₄, MeOH; (ii) TFA, CH₂Cl₂; (iii) K₂CO₃, MgSO₄, HCHO, CH₂Cl₂.

needed to verify such a hypothesis, as the decreased activity of **13** and **14** could also possibly be due to molecular instability (the hemiaminal ether E-ring).

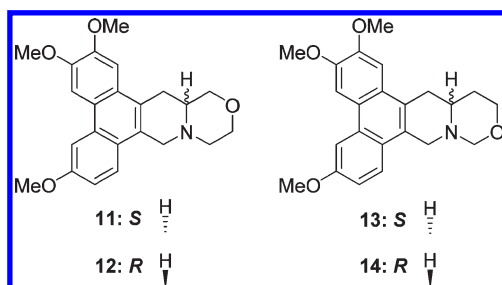
Our study of O incorporation in antofine/cryptopleurine-type compounds was also extended to the previously reported 7-membered E-ring analogue **15**.²⁹ Its O-containing analogue **16** was synthesized using procedures similar to those for **11** (Scheme 5). First, the aldehyde of **9** was reduced to a hydroxymethyl group followed by the removal of Boc. The resulting amino intermediate was then reacted with chloroacetyl chloride at 0 °C to provide the chloroacetamide, which was subjected to ring closure and subsequent reduction of the amide carbonyl to a methylene with BMS to give compound **16** in 24% yield over five steps.

When tested in parallel for cytotoxicity, both **15** and **16** were more active against A549 and HCT-8 cancer cell lines than

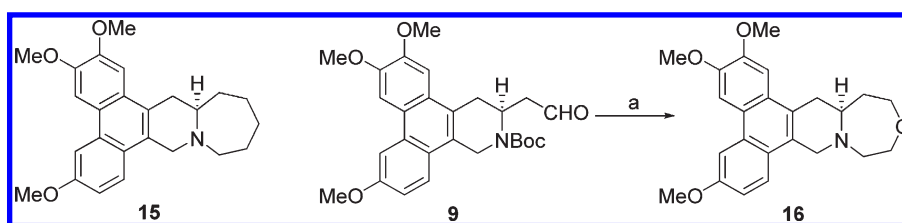
against DU145 and KB (Table 5). Compound **16** was slightly more active than **15** against DU145 and KB cell proliferation, while it was slightly less active against A549 and HCT-8. These results suggested that the remarkable cell-line selectivity of **15** was somewhat decreased by introducing an oxygen atom at C13. Nevertheless, both analogues exhibited strong potency against the HCT-8 cell line, which indicated that phenanthroindolizidine and phenanthroquinolizidine derivatives with a 7-membered E-ring have a new and interesting structural scaffold and could have a great potential for further development as selective anticancer agents.

In consideration of the impressive cytotoxicity, we next aimed our study at the potential mechanism(s) of action of the representative analogues **11** and **15**, as well as *R*-antofine. Our preliminary cDNA microarray data indicated that *R*-antofine had a profound influence on the major replication initiation complex ORC (origin recognition complex) and MCM (DNA replication licensing factor) in early S phase. The DNA replication licensing factors Cdt1 (DNA replication factor) and CDC6 (cell division control protein 6) were also up-regulated in a dose- or time-dependent manner when CL1–5 cells were exposed to *R*-antofine for 24 and 48 h, as confirmed by RT-PCR (0.01 $\mu\text{g}/\text{mL}$, Figure 2) and Western blot analysis (Figure 3). These data indicated that *R*-antofine promotes dysregulation of DNA replication in lung cancer cells. However, it is not clear whether the cytotoxic effect of *R*-antofine is directly correlated with promoting dysregulation of DNA replication. In general, the effects of **11** and **15** were not significant, falling in between those produced by *R*-antofine and control. An in-depth investigation on diverse cell events should be helpful for further clarification of their mechanism of action. Obviously, the difference in the E-ring structure is involved in these observed effects, and the E-ring is not totally indispensable.

Compound **11** was then selected for an *in vivo* study in mice against HT-29 human colorectal adenocarcinoma xenograft. Mice in group 1 received the vehicle and served as the control for all treatment groups. The median time to end point (TTE) for mice in the control group was 16.3 days with a range of

Table 4. GI₅₀ Values of Analogues 11–14 against Four Cancer Cell Lines

compd.	config.	A549	DU145	KB	HCT-8
11	S	23 ± 5 nM	67 ± 10 nM	37 ± 9 nM	9 ± 5 nM
12	R	13.95 ± 4.74 μM	7.05 ± 1.25 μM	6.68 ± 1.52 μM	3.45 ± 0.56 μM
13	S	1.79 ± 0.27 μM	1.82 ± 0.31 μM	1.66 ± 0.33 μM	1.45 ± 0.24 μM
14	R	1.37 ± 0.29 μM	1.29 ± 0.36 μM	1.10 ± 0.28 μM	1.26 ± 0.20 μM
crypto-pleurine	R	1.38 ± 0.56 nM	1.59 ± 0.53 nM	1.51 ± 0.33 nM	1.09 ± 0.20 nM

Scheme 5^a

^a Reagents and conditions: (a) (i) NaBH₄, MeOH; (ii) TFA, CH₂Cl₂; (iii) ClCH₂COCl, Et₃N, CH₂Cl₂, 0 °C; (iv) NaH, THF, reflux; (v) BMS, THF, 24% for 5 steps.

Table 5. GI₅₀ Values of Compounds 15 and 16

compd.	config.	A549 (nM)	DU145 (nM)	KB (nM)	HCT-8 (nM)
15	R	25 ± 5	179 ± 36	102 ± 19	10 ± 3
16	S	41 ± 9	119 ± 33	68 ± 10	20 ± 6

13.8–21.9 days. Compound 11, i.v. at 20 mg/kg (qd to end), produced a median TTE of 21.3 days and caused 1.1% maximum group body weight loss on day 12, indicating statistically significant antitumor activity ($P < 0.05$) and no obvious toxicity. When dosed i.v./i.p. at 20 mg/kg (bid to end), 11 produced a median TTE of 20.9 days and caused 7.2% maximum group body weight loss occurring on day 19. One tumor remained in the study on day 29, and one treatment-related (TR) death occurred on day 20 (Figures 4 and 5). When dosing frequency was increased, no improved efficacy was observed. Interestingly, a similar phenomenon was also reported in previous studies. For instance, the effectiveness of phenanthroindolizidine analogues with C14-OH was found to be highly schedule dependent, e.g., the therapeutic index of DCB-3503 may be lost if given daily instead of every three days.³⁴ Therefore, a more rationally designed dosing regimen is being investigated in order for the compounds to exert their best tumor inhibitory effects and meanwhile reduce toxicity that could result from unnecessary repetitive dosing. Moreover, we tested compound 11 against human umbilical vein endothelial cells (HUVECs, normal cells), and the results indicated that the cytotoxicity of

R-cryptopleurine was reduced by 30-fold through our modification, as shown in Figure 6 (GI₅₀ 320 nM vs 11 nM). Such improved selectivity against cancer cells over normal cells demonstrates that our newly synthesized analogues can potentially reduce unwanted side effects *in vivo*. In summary, compound 11 exhibited potent *in vitro* anticancer activity with improved cell line selectivity and moderate antitumor activity against HT-29 human colorectal adenocarcinoma in male nude-athymic mice at a dose of 20 mg/kg without causing obvious toxicity.

CONCLUSIONS

New synthetic antofine and cryptopleurine analogues with varied E-ring size or heteroatom incorporation were designed and prepared. Two analogues, 11 and 16, were the most active compounds against tested cancer cell lines, with interestingly improved selectivity against HCT-8 cell growth. Mechanistic studies indicated that R-antofine is capable of promoting dysregulation of DNA replication in early S phase, whereas no similar results were found for compounds 11 and 15. It is still unclear as to how this activity correlates with the potent cytotoxicity of antofine, and further investigation is ongoing. In our *in vivo* antitumor study, we found that 11 had improved activity on HUVECs and moderate antitumor effect on human HT-29 adenocarcinoma xenograft in mice. However, further studies in other tumor models are warranted to find out which type of tumor affords the most sensitivity and what treatment protocol

provides the best therapeutic index. Moreover, compound **16** appears to be an interesting analogue that necessitates in-depth investigation, and results will be reported in due course. Additionally, CNS toxicity will also be explored in the future.

EXPERIMENTAL SECTION

All chemicals were used as purchased. Melting points were measured using a Fisher Johns melting apparatus without correction. Proton nuclear magnetic resonance (^1H NMR) spectra were measured on a

300 MHz Gemini or a Varian Inova (400 MHz) NMR spectrometer with TMS as the internal standard. The solvent used was CDCl_3 unless otherwise indicated. Mass spectra were recorded on a Shimadzu-2010 LC/MS/MS instrument equipped with a TurboIonsSpray ion source. All final target compounds were characterized and determined as at least >95% pure by analytical HPLC.

(*S*)-*N*-Boc-(6,7,10-trimethoxy-1,2,3,4-tetrahydrodibenzo[*f,h*]isoquinolin-3-yl)methanol (**2**). (Boc) $_2\text{O}$ (3.14 g, 14.40 mmol) was added to the amino-alcohol (4.24 g, 12 mmol) in 100 mL of CH_2Cl_2 and Et_3N (6 mL), and the mixture was stirred for 2 h. HCl (50 mL, 1 N) was added, and the organic layer was separated, washed with sat. NaHCO_3 and brine, and dried over MgSO_4 . Column chromatography eluting with $\text{CH}_2\text{Cl}_2/\text{MeOH}$ gave 5.20 g of compound **2** as a white solid. Yield: 95.6%; mp 105–107 °C; $[\alpha]^{23}_{\text{D}} = 85.5^\circ$ (*c* 0.42, CHCl_3). ^1H NMR (300 MHz, CDCl_3): δ 7.89 (s, 2H), 7.81 (d, *J* = 9.0 Hz, 1H), 7.28 (s, 1H), 7.22 (d, *J* = 8.7 Hz, 1H), 5.29 (br s, 1H), 4.84 (m, 1H), 4.61 (br s, 1H), 4.09 (s, 3H), 4.05 (s, 3H), 4.01 (s, 3H), 3.73–3.62 (m, 2H), 3.27 (dd, *J* = 16.5 Hz, *J* = 6.3 Hz, 1H), 3.18 (t, *J* = 16.5 Hz, 1H), 1.55 (s, 9H). ^{13}C NMR (75 MHz, CDCl_3): δ 157.9, 156.2, 149.7, 148.8, 130.4, 126.7, 124.0, 123.9, 123.8, 123.4, 122.8, 115.2, 105.1, 104.2, 104.0, 80.6, 62.7, 56.2, 56.0, 55.7, 50.6, 41.0, 28.6 (3 × C), 26.5. ESI-HRMS ($[\text{M} + \text{H}]^+$) calcd for $\text{C}_{26}\text{H}_{32}\text{NO}_6$ 454.2230; found, 454.2246.

General Procedures for the Synthesis of 12*N*-Substituted-12-aza-antofine (3a–l). The aldehyde was obtained using the same procedure as that for compound **8**. Various amines were reacted with the aldehyde in MeOH, followed by the addition of HOAc and NaBH_3CN , which was stirred at r.t. for 4 h. Saturated NaHCO_3 was added to quench the reaction, and CH_2Cl_2 was used for extraction. The residue was quickly purified through a column, and TFA was used to remove the Boc group. Then TFA was removed by evaporation, and the residue was dissolved in CH_2Cl_2 (10 mL), to which K_2CO_3 (100 mg) and MgSO_4 (0.5 g) were added, followed by HCHO (37%, 0.1 mL). The mixture was stirred at r.t. overnight. Chromatography gave light yellow to white solids. Yield: 40%–80%.

(*S*)-*tert*-Butyl-6,7,10-trimethoxy-3-((2-methoxy-2-oxoethylamino)methyl)-3,4-dihydrodibenzo[*f,h*]isoquinoline-2(1*H*)-carboxylate (**4**). The Boc-aldehyde was obtained using the same procedure as that used for compound **8**. Glycine methyl ester

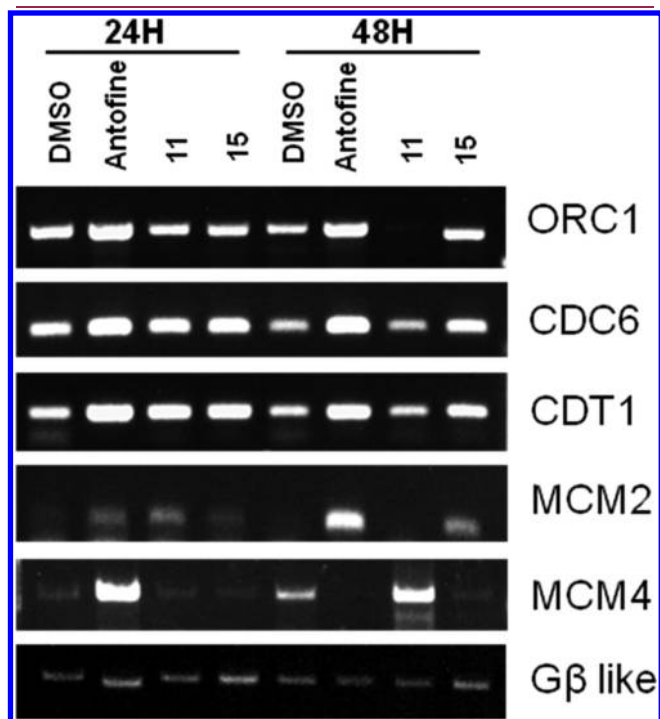


Figure 2. RT-PCR results of *R*-antofine, **11**, and **15** at 0.01 $\mu\text{g}/\text{mL}$ on major DNA replication complexes in CL1–5 cells at 24 and 48 h.

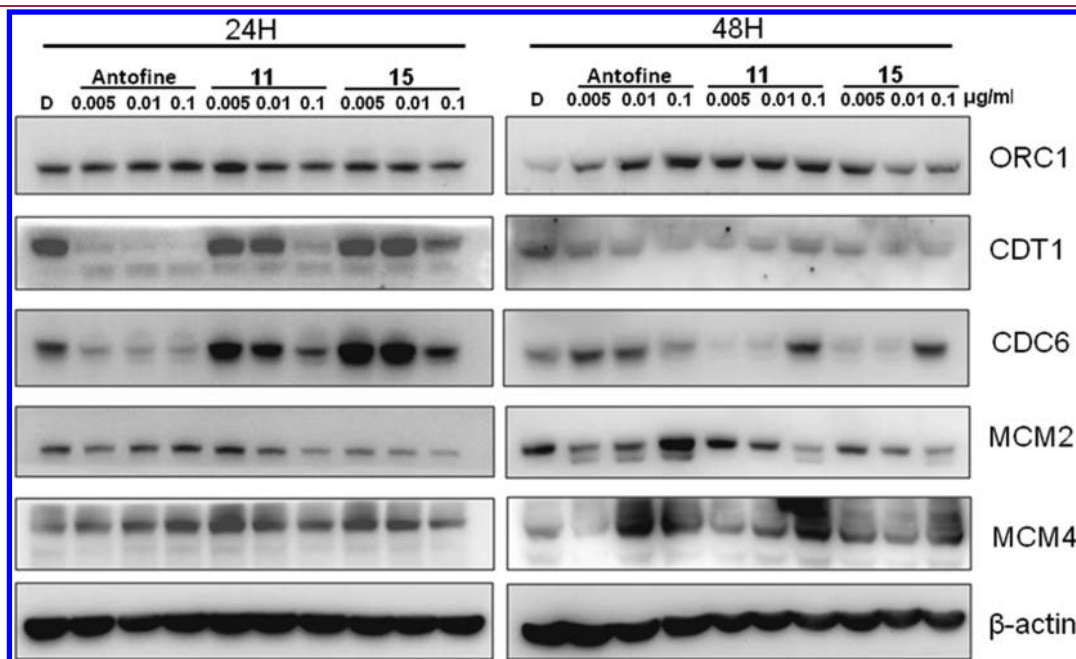


Figure 3. Western blot analysis of *R*-antofine, **11**, and **15** on major DNA replication complexes in CL1–5 cells at 24 and 48 h.

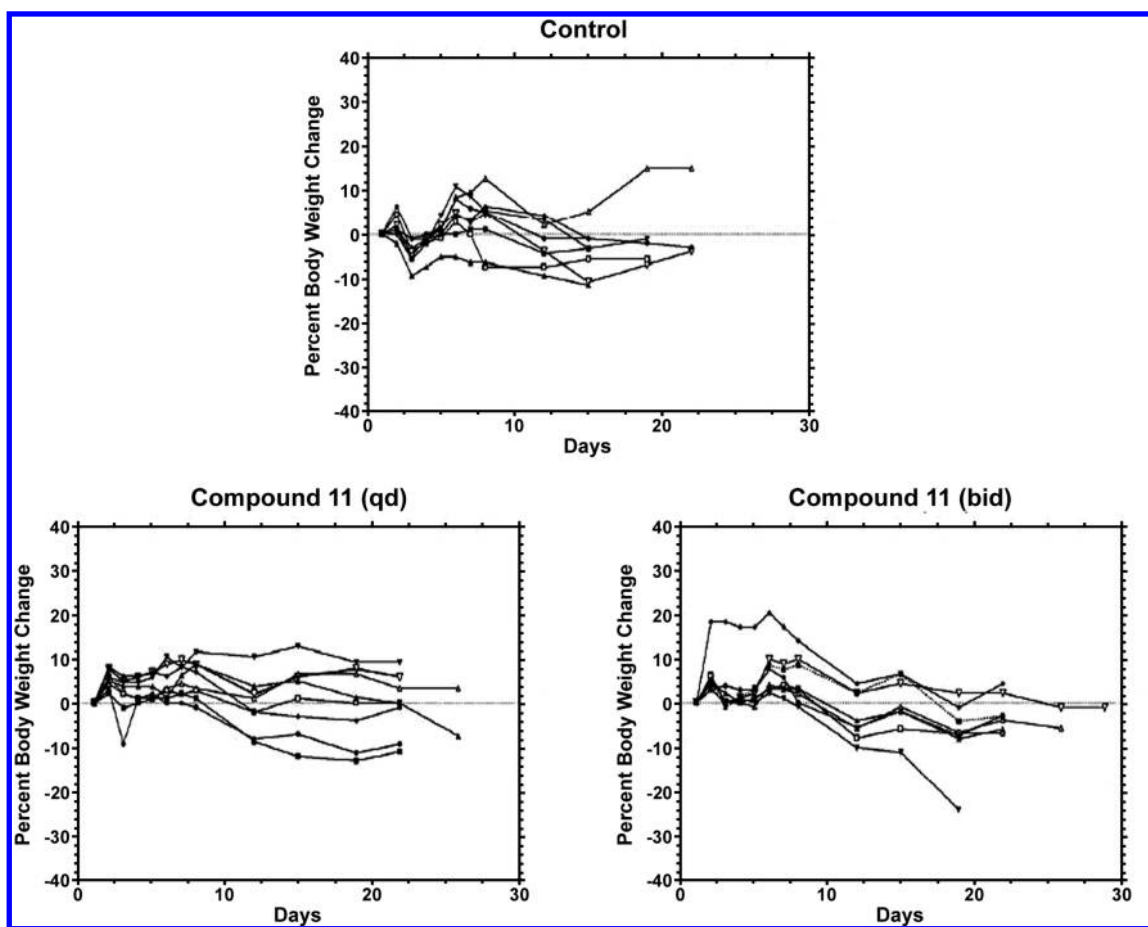


Figure 4. Individual animal body weight change for control and treatment groups.

hydrochloride (314 mg, 2.5 mmol) and Et_3N (0.35 mL, 2.5 mmol) were added to the aldehyde in MeOH (30 mL), which was stirred for 0.5 h. Then HOAc (0.70 mL, 12 mmol) and NaBH_3CN (165 mg, 2.5 mmol) were added. The mixture was stirred for 2 h until all the aldehyde disappeared. Saturated NaHCO_3 was used to quench the reaction, and CH_2Cl_2 was used for extraction, and washed with brine, dried over MgSO_4 . Chromatography gave 635 mg of compound 4 as a white solid. Yield: 61% over two steps. mp 78–80 °C; $[\alpha]_D^{23} = 91.6^\circ$ (*c* 0.37, CHCl_3). $^1\text{H NMR}$ (400 MHz, CDCl_3): δ 7.92 (s, 1H), 7.91 (d, *J* = 2.4 Hz, 1H), 7.87 (brs, 1H), 7.44–7.42 (m, 2H), 7.29 (s, 1H), 7.25–7.23 (m, 1H), 5.40–5.29 (m, 1H), 4.92–4.78 (m, 1H), 4.56 (m, 1H), 4.11 (s, 3H), 4.05 (s, 3H), 4.02 (s, 3H), 3.66 (s, 3H), 3.47–3.36 (m, 2H), 3.27 (dd, *J* = 16.4 Hz, *J* = 6.4 Hz, 1H), 3.14 (d, *J* = 16.4 Hz, 1H), 2.81 (dd, *J* = 12.0 Hz, *J* = 8.8 Hz, 1H), 2.64 (dd, *J* = 12.0 Hz, *J* = 6.4 Hz, 1H), 1.54 (s, 9H). ESI MS *m/z* 525.20 ($\text{M} + \text{H}$) $^+$.

(S)-13N-Boc-11-oxo-13-aza-cryptopleurine (5). The ester (635 mg, 1.21 mmol) was dissolved in HCl (1.25 M in methanol, 15 mL), which was stirred at 50 °C for 1 h. The solvent was removed. Thirty milliliters of MeOH and Et_3N (0.3 mL) was added. The mixture was stirred at r.t. for 2 h. After normal workup, chromatography afforded 404 mg of ring-closed intermediate as a white solid. Using a procedure similar to that for compound 2, the intermediate was protected by $(\text{Boc})_2\text{O}$ to give 456 mg of 5 as a white solid. Yield: 76% over three steps. mp 125–127 °C; $[\alpha]_D^{23} = -202.8^\circ$ (*c* 0.50, CHCl_3). $^1\text{H NMR}$ (400 MHz, CDCl_3): δ 7.89 (s, 1H), 7.88 (d, *J* = 2.8 Hz, 1H), 7.87 (d, *J* = 9.2 Hz, 1H), 7.23 (dd, *J* = 9.2 Hz, *J* = 2.8 Hz, 1H), 7.19 (s, 1H), 5.88 (d, *J* = 17.2 Hz, 1H), 4.49 (d, *J* = 17.2 Hz, 1H), 4.40 (d, *J* = 18.0 Hz, 1H), 4.10 (s, 4H), 4.05 (s, 4H), 4.01 (s, 3H), 3.87–3.77 (m, 2H), 3.16 (m, 2H), 1.51 (s, 9H). ESI MS *m/z* 493.10 ($\text{M} + \text{H}$) $^+$, 985.20 ($2\text{M} + \text{H}$) $^+$.

(S)-13N-Boc-13-aza-cryptopleurine (6). To a solution of the amide (456 mg, 0.93 mmol) in THF (30 mL) was added BMS (2 M in THF, 2.79 mL), which was stirred at r.t. overnight. Five milliliters of MeOH was added, and the mixture was refluxed for 1 h. Chromatography afforded 400 mg of 6 as a white solid. Yield: 90%. mp 116–118 °C; $[\alpha]_D^{23} = -182.5^\circ$ (*c* 0.28, CHCl_3). $^1\text{H NMR}$ (400 MHz, CDCl_3): δ 7.88–7.87 (m, 2H), 7.76 (d, *J* = 8.8 Hz, 1H), 7.20 (s, 1H), 7.19 (dd, *J* = 8.8 Hz, *J* = 2.8 Hz, 1H), 4.44 (d, *J* = 15.2 Hz, 1H), 4.29 (m, 1H), 4.11 (m, 1H), 4.09 (s, 3H), 4.05 (s, 3H), 4.00 (s, 3H), 3.66 (d, *J* = 15.2 Hz, 1H), 3.15 (m, 2H), 3.04 (dd, *J* = 16.4 Hz, *J* = 3.2 Hz, 1H), 2.87 (m, 1H), 2.80 (dd, *J* = 16.4 Hz, *J* = 11.8 Hz, 1H), 2.57–2.52 (m, 1H), 2.45 (dt, *J* = 12.0 Hz, 3.2 Hz, 1H). ESI MS *m/z* 479.10 ($\text{M} + \text{H}$) $^+$.

General Procedures for the Synthesis of 13N-Substituted-13-aza-cryptopleurine (7a–q). (a) 13N-Boc-13-aza-cryptopleurine 6 was stirred in HCl/MeOH for 2 h before the solvent was removed *in vacuo*. The solid was collected and washed sequentially with cold MeOH and ether. Then the solid was dissolved in 10 mL of anhydrous CH_2Cl_2 and Et_3N (0.1 mL), to which RCOCl was added at 0 °C. The mixture was stirred at r.t. for 4 h before 1 N HCl was added. After routine workup, chromatography afforded from light orange to white solids. Yield: 70%–80%. (b) The same procedures (reductive amination) as those for compound 4 were used. Yield: 50%–80%.

(S,E/Z)-6,7,10-Trimethoxy-3-(2-methoxyvinyl)-1,2,3,4-tetrahydrodibenzo[*f,h*]isoquinoline (8). *N*-Boc-alcohol 2 (1.812 g, 4 mmol) was dissolved in CH_2Cl_2 (50 mL) and Et_3N (1.95 mL, 14 mmol) at 0 °C, to which $\text{Py} \cdot \text{SO}_3$ (2.23 g, 14 mmol) in 10 mL of DMSO was added dropwise. The ice bath was then removed, and the mixture was stirred at r.t. until 2 disappeared by TLC. HCl (1 N) was added, and the

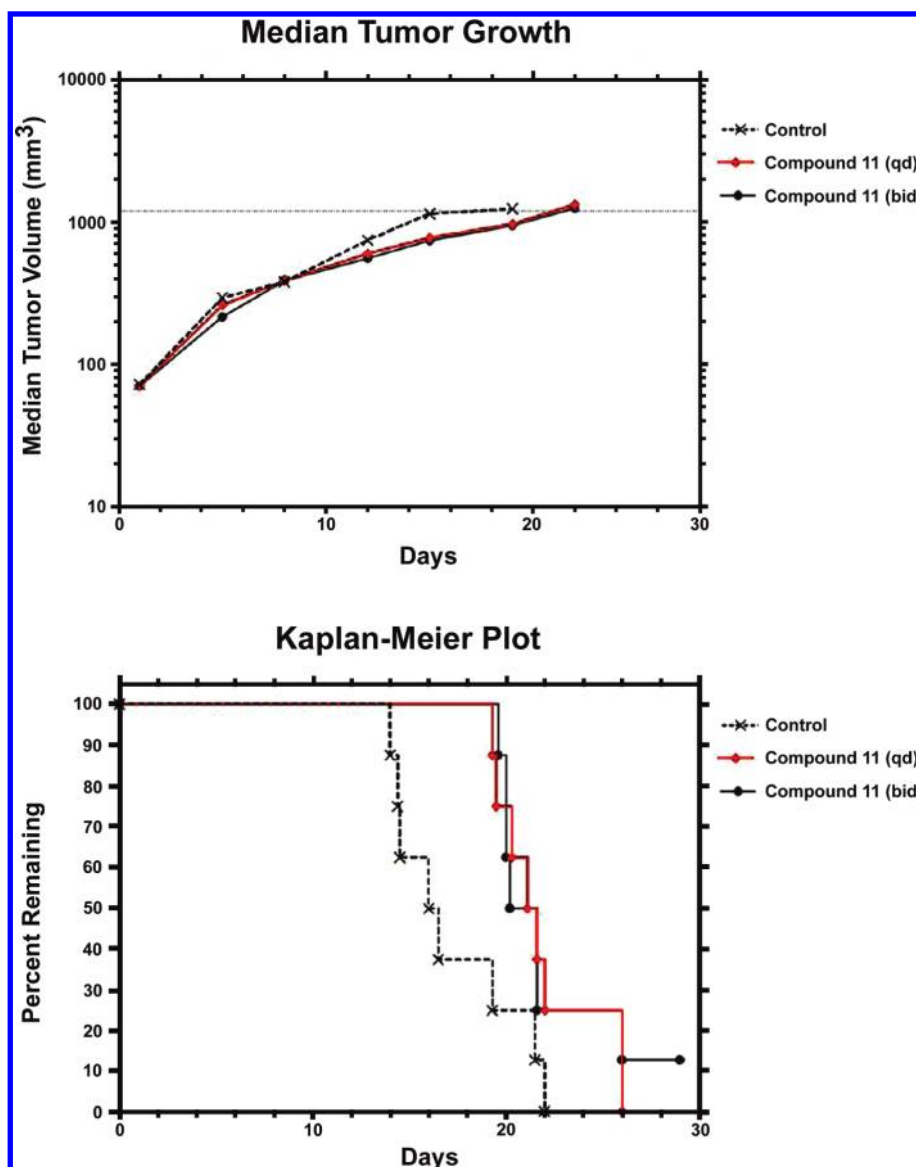


Figure 5. *In vivo* antitumor activity of compound 11.

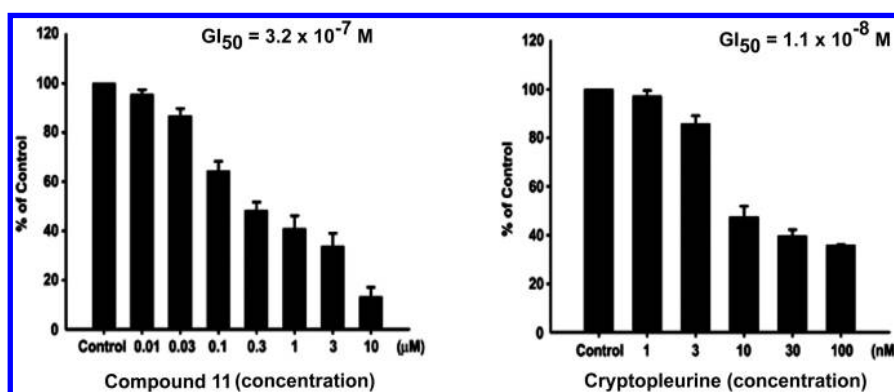


Figure 6. Comparison of compound 11 and *R*-cryptopleurine against human umbilical vein endothelial cells (HUVECs).

organic layer was then separated and washed with sat. NaHCO₃, brine, and dried over MgSO₄. In another flask, Ph₃P⁺CH₂OMeCl⁻ (2.74 g, 8 mmol) was added to KO^tBu (875 mg, 7.8 mmol) at 0 °C under N₂,

which was stirred for 0.5 h. The aldehyde in 20 mL of CH₂Cl₂ was added dropwise, followed by the removal of the ice bath. The reaction was kept for 2–3 h before sat. NH₄Cl was poured into the mixture. CH₂Cl₂ was

used for extraction, and the organic layers were washed with sat. NaHCO_3 and brine, dried over MgSO_4 . Chromatography afforded 1.5 g of compound **8** as a light yellow solid. Yield: 78% ($Z/E = 1/2.5$) for two steps. mp 150–152 °C; $[\alpha]^{23}_{\text{D}} = 108.1^\circ$ (c 0.59, CHCl_3). $^1\text{H NMR}$ (400 MHz, CDCl_3 , $E/Z = 2.5:1$): δ 7.94–7.91 (m, 2H), 7.88 (d, $J = 9.2$ Hz, 1H), 7.29 (s, 1H), 7.26–7.22 (m, 1H), 6.30 (d, $J = 12.8$ Hz, 0.68H, E isomer), 5.86 (dd, $J = 6.4$ Hz, $J = 1.6$ Hz, 0.28 Hz, Z isomer), 5.72 (m, 0.31H, Z isomer), 5.30–5.25 (d, $J = 16.8$ Hz, 1H+0.67H, E isomer), 4.80 (dd, $J = 12.8$ Hz, $J = 8.4$ Hz, 0.71 H, E isomer), 4.59 (d, $J = 17.2$ Hz, 1H), 4.42 (dd, $J = 8.0$ Hz, $J = 6.4$ Hz, 0.29H, Z isomer), 4.12–4.11 (m, 3H), 4.05–4.04 (m, 3H), 4.03–4.02 (m, 3H), 3.62 (s, 0.71H, Z isomer), 3.44–3.32 (m, 1H), 3.36 (s, 2H, E isomer), 3.13 (d, $J = 16.0$ Hz, 1H), 1.55 (s, 9H). ESI MS m/z 480.05 ($M + H$) $^+$.

(S)-2-(6,7,10-Trimethoxy-1,2,3,4-tetrahydrobenzo[*f,h*]isoquinolin-3-yl)acetaldehyde (9). Compound **8** (1.5 g, 3.12 mmol) was dissolved in THF (50 mL) and H_2O (5 mL), to which $\text{Hg}(\text{OAc})_2$ (3.0 g, 9.36 mmol) was added at 0 °C. Then the ice bath was removed, and the mixture was stirred overnight. Freshly prepared sat. KI (50 mL) was added dropwise at 0 °C for 10 min, and CH_2Cl_2 was used for extraction. The organic layers were collected and washed with brine, dried over MgSO_4 . Chromatography furnished 1.09 g of compound **9** as a light yellow foam. Yield: 75%. mp 98–100 °C; $[\alpha]^{23}_{\text{D}} = 94.4^\circ$ (c 0.68, CHCl_3). $^1\text{H NMR}$ (400 MHz, CDCl_3): δ 9.79 (s, 1H), 7.93 (s, 1H), 7.91 (d, $J = 2.4$ Hz, 1H), 7.85 (brs, 1H), 7.26–7.24 (m, 2H), 5.38–5.29 (m, 2H), 4.58 (d, $J = 16.0$ Hz, 1H), 4.11 (s, 3H), 4.05 (s, 3H), 4.02 (s, 3H), 3.38 (dd, $J = 16.0$ Hz, $J = 6.4$ Hz, 1H), 3.12 (d, $J = 16.4$ Hz, 1H), 2.70–2.59 (m, 2H), 1.53 (s, 9H). ESI MS m/z 466.10 ($M + H$) $^+$, 488.15 ($M + \text{Na}$) $^+$.

General Procedures for the Synthesis of 12*N*-Substituted-12-aza-cryptopleurine (10a–j). Similar procedures as those used for compound **3a–I** were used. Yield: 50%–70%.

(S)-13-Oxa-cryptopleurine (11) and (R)-13-Oxa-cryptopleurine (12). Compound **2** (177 mg, 0.5 mmol) was suspended in dry CH_2Cl_2 (15 mL) and Et_3N (0.14 mL, 1.00 mmol) at 0 °C, to which chloroacetyl chloride (40 μL , 0.50 mmol) in 1 mL of CH_2Cl_2 was slowly added dropwise. The mixture was stirred at 0 °C for 5 h before 1 N HCl was added. The organic layer was separated and washed with sat. NaHCO_3 and brine, dried over MgSO_4 . CH_2Cl_2 was removed, and the residue was dissolved in anhydrous THF (5 mL), to which NaH (2.1 equiv) was added at r.t. followed by reflux for 2 h. Saturated NH_4Cl was added, and CH_2Cl_2 was used for extraction. After workup, the organic layer was dried over MgSO_4 . Then the residue was dissolved in 10 mL of anhydrous THF, and BMS (1.50 mL, 6 mmol) was added, which was stirred at r.t. overnight. MeOH (5 mL) was added, and the mixture was refluxed for 1 h. Chromatography gave 73 mg of **11** as a white solid. Yield: 38.5% for three steps; white solid; mp 199–201 °C; $[\alpha]^{23}_{\text{D}} = -134.6^\circ$ (c 0.52, CHCl_3). $^1\text{H NMR}$ (300 MHz, CDCl_3): δ 7.86–7.85 (m, 2H), 7.74 (d, $J = 9.0$ Hz, 1H), 7.18 (dd, $J = 9.0$ Hz, $J = 2.4$ Hz, 1H), 7.14 (s, 1H), 4.39 (d, $J = 15.6$ Hz, 1H), 4.12 (m, 2H), 4.08 (s, 3H), 4.03 (s, 3H), 4.00 (s, 3H), 3.91–3.83 (m, 1H), 3.66 (d, $J = 15.6$ Hz, 1H), 3.51 (dd, $J = 11.1$ Hz, $J = 9.0$ Hz, 1H), 3.06 (d, $J = 11.7$ Hz, 1H), 2.91–2.87 (m, 1H), 2.76–2.59 (m, 3H). ESI MS m/z 380.05 ($M + H$) $^+$. For **12**: mp 196–198 °C; $[\alpha]^{23}_{\text{D}} = 139.6^\circ$ (c 0.26, CHCl_3). $^1\text{H NMR}$ (300 MHz, CDCl_3): δ 7.90–7.89 (m, 2H), 7.78 (d, $J = 9.0$ Hz, 1H), 7.20 (dd, $J = 9.0$ Hz, $J = 2.7$ Hz, 1H), 7.20 (s, 1H), 4.44 (d, $J = 15.6$ Hz, 1H), 4.17–4.08 (m, 1H), 4.10 (s, 3H), 4.05 (s, 3H), 4.01 (s, 3H), 4.04–4.00 (m, 1H), 3.92–3.84 (m, 1H), 3.72 (d, $J = 15.3$ Hz, 1H), 3.54 (dd, $J = 11.1$ Hz, $J = 9.0$ Hz, 1H), 3.09 (d, $J = 11.4$ Hz, 1H), 2.98–2.94 (m, 1H), 2.77–2.61 (m, 3H). $^{13}\text{C NMR}$ (75 MHz, CDCl_3): δ 157.5, 149.4, 148.4, 130.2, 126.4, 125.1, 124.1, 123.6, 123.4, 123.3, 115.0, 104.7, 103.8, 103.6, 72.3, 67.4, 56.1, 56.0, 55.9, 55.5, 55.1, 54.4, 28.5. ESI MS m/z 380.05 ($M + H$) $^+$.

(S)-12-Oxa-cryptopleurine (13) and (R)-12-Oxa-cryptopleurine (14). Aldehyde **9** (100 mg, 0.21 mmol) was dissolved in MeOH, to which NaBH_4 (19 mg, 0.50 mmol) was added in one portion. The mixture was stirred for 1 h, and sat. NaHCO_3 was added. After normal

workup, 80 mg of white solid was obtained, which was used without further purification. The residue was dissolved in CH_2Cl_2 (10 mL), to which MgSO_4 , K_2CO_3 , and HCHO were sequentially added. The mixture was stirred overnight. After workup, chromatography gave 32 mg of **13** as a white solid. Yield: 40% for two steps; light yellow solid; mp 195–197 °C; $[\alpha]^{23}_{\text{D}} = -56.8^\circ$ (c 0.60, CHCl_3). $^1\text{H NMR}$ (300 MHz, CDCl_3): δ 7.89–7.88 (m, 2H), 7.75 (d, $J = 9.3$ Hz, 1H), 7.22 (s, 1H), 7.19 (dd, $J = 9.0$ Hz, $J = 2.7$ Hz, 1H), 4.79 (d, $J = 8.4$ Hz, 1H), 4.41 (d, $J = 15.3$ Hz, 1H), 4.19 (dd, $J = 11.1$ Hz, $J = 5.1$ Hz, 1H), 4.10 (s, 3H), 4.05 (s, 3H), 4.03 (m, 1H), 4.01 (s, 3H), 3.75–3.65 (m, 2H), 3.17 (dd, $J = 15.9$ Hz, $J = 3.6$ Hz, 1H), 2.95–2.80 (m, 2H), 2.06–1.92 (m, 1H), 1.74 (m, 1H); ESI MS m/z 380.05 ($M + H$) $^+$. For **14**: mp 191–192 °C; $[\alpha]^{23}_{\text{D}} = 51.2^\circ$ (c 0.60, CHCl_3). $^1\text{H NMR}$ (300 MHz, CDCl_3): δ 7.87–7.86 (m, 2H), 7.73 (d, $J = 9.0$ Hz, 1H), 7.20 (s, 1H), 7.18 (dd, $J = 9.6$ Hz, $J = 3.0$ Hz, 1H), 4.77 (d, $J = 8.1$ Hz, 1H), 4.38 (d, $J = 15.3$ Hz, 1H), 4.18 (dd, $J = 11.1$ Hz, $J = 4.8$ Hz, 1H), 4.09 (s, 3H), 4.04 (s, 3H), 3.99 (s, 3H), 3.98 (d, $J = 8.1$ Hz, 1H), 3.73–3.61 (m, 2H), 3.13 (dd, $J = 15.9$ Hz, $J = 3.6$ Hz, 1H), 2.91–2.72 (m, 2H), 2.02–1.90 (m, 1H), 1.72–1.67 (m, 1H). $^{13}\text{C NMR}$ (75 MHz, CDCl_3): δ 157.7, 149.6, 148.5, 130.3, 126.6, 124.7, 124.2, 123.8, 123.7, 123.6, 115.0, 104.9, 104.5, 103.9, 86.5, 68.1, 56.1, 56.0, 55.7, 55.4, 48.0, 33.5, 31.3. ESI MS m/z 380.05 ($M + H$) $^+$.

Compound 16. Aldehyde **9** (140 mg, 0.30 mmol) was dissolved in MeOH, to which NaBH_4 (76 mg, 2 mmol) was added. The resulting mixture was stirred at r.t. for 1 h before sat. NaHCO_3 was added. The mixture was extracted with CH_2Cl_2 , and the organic layers were combined, washed with brine, and dried over Na_2SO_4 . Then the solvent was removed under reduced pressure and redissolved in TFA/ CH_2Cl_2 (1:1, 10 mL), which was stirred for 0.5 h. The mixture was concentrated to remove TFA. The residue was subject to treatment with chloroacetyl chloride, and the rest of the synthesis was similar to that of compound **11**. After chromatography, 37 mg of **16** was obtained as a light yellow solid in 24% yield over five steps. mp 183–185 °C; $[\alpha]^{23}_{\text{D}} = -114.7^\circ$ (c 0.19, CHCl_3). $^1\text{H NMR}$ (400 MHz, CDCl_3): δ 7.90 (s, 1H), 7.88 (d, $J = 2.4$ Hz, 1H), 7.75 (d, $J = 9.2$ Hz, 1H), 7.24 (s, 1H), 7.19 (dd, $J = 9.2$ Hz, $J = 2.4$ Hz, 1H), 4.43 (d, $J = 15.2$ Hz, 1H), 4.10 (s, 3H), 4.05 (m, 4H), 4.01 (m, 4H), 3.98–3.90 (m, 3H), 3.20–3.13 (m, 1H), 3.08–3.01 (m, 3H), 2.96–2.91 (m, 1H), 2.25–2.19 (m, 1H), 2.17–2.11 (m, 1H). $^{13}\text{C NMR}$ (100 MHz, CDCl_3): δ 157.7, 149.6, 148.6, 130.3, 126.9, 126.6, 125.4, 124.2, 123.9, 123.7, 115.1, 104.9, 104.1, 104.0, 69.9, 66.5, 59.0, 57.6, 57.0, 56.2, 56.1, 55.7, 36.7, 35.5. ESI MS m/z 394.10 ($M + H$) $^+$.

■ ASSOCIATED CONTENT

Supporting Information. Compound data for **3a–I**, **7a–q**, and **10a–j**, biological studies, and HPLC analysis of final compounds. This material is available free of charge via the Internet at <http://pubs.acs.org>.

■ AUTHOR INFORMATION

Corresponding Author

* (Q.S.) Phone: 919-843-6325. Fax: 919-966-3893. E-mail: qshil@email.unc.edu. (P.-C.Y.) Phone: 886-2-2356-2185. Fax: 886-2-2322-4793. E-mail: pcyang@ntu.edu.tw. (K.-H.L.) Phone: 919-962-0066. Fax: 919-966-3893. E-mail: khlee@unc.edu.

■ ACKNOWLEDGMENT

This study was supported by grant CA17625-32 from the National Cancer Institute awarded to K.H.L. and grant DOH98-TD-G-111-007 from the National Research Program for Genomic Medicine awarded to P.C.Y. This study was also supported in part by the Department of Health Cancer Research Center of Excellence (DOH-100-TD-C-111-05).

■ ABBREVIATIONS USED

MOA, mechanism of action; NCI, National Cancer Institute; HIF-1, hypoxia-inducible factor 1; TS, thymidylate synthase; DHFR, dihydrofolate reductase; AP-1, activator protein-1; CRE, cAMP response element; CDK, cyclin-dependent kinase; CNS, central neural system; SAR, structure–activity relationship; BBB, blood–brain barrier; PSA, polar surface area; ORC, origin recognition complex; CDC6, cell division control protein 6; RT-PCR, reverse transcription polymerase chain reaction; HUVECs, human umbilical vein endothelial cells

■ REFERENCES

- (1) Gellert, E. The indolizidine alkaloids. *J. Nat. Prod.* **1982**, *45* (1), 50–73.
- (2) Xi, Z.; Zhang, R.; Yu, Z.; Ouyang, D. The interaction between tylophorine B and TMV RNA. *Bioorg. Med. Chem. Lett.* **2006**, *16* (16), 4300–4304.
- (3) Wang, K.; Su, B.; Wang, Z.; Wu, M.; Li, Z.; Hu, Y.; Fan, Z.; Mi, N.; Wang, Q., Synthesis and antiviral activities of phenanthroindolizidine alkaloids and their derivatives. *J. Agric. Food Chem.* **2010**, *58* (5), 2703–2709.
- (4) Baumgartner, B.; Erdelmeier, C. A. J.; Wright, A. D.; Rali, T.; Sticher, O. An antimicrobial alkaloid from *Ficus septica*. *Phytochemistry* **1990**, *29* (10), 3327–3330.
- (5) Bhutani, K. K.; Sharma, G. L.; Ali, M. Plant based antiameobic drugs; Part I. Antiameobic activity of phenanthroindolizidine alkaloids; common structural determinants of activity with emetine. *Planta Med.* **1987**, *53* (6), 532–536.
- (6) Banwell, M. G.; Bezos, A.; Burns, C.; Kruszelnicki, I.; Parish, C. R.; Su, S.; Sydnes, M. O. C8c-C15 monoseco-analogues of the phenanthroquinolizidine alkaloids julandine and cryptopleurine exhibiting potent anti-angiogenic properties. *Bioorg. Med. Chem. Lett.* **2006**, *16* (1), 181–185.
- (7) Yang, C.-W.; Chen, W.-L.; Wu, P.-L.; Tseng, H.-Y.; Lee, S.-J. Anti-inflammatory mechanisms of phenanthroindolizidine alkaloids. *Mol. Pharmacol.* **2006**, *69* (3), 749–758.
- (8) Yang, C.-W.; Chuang, T.-H.; Wu, P.-L.; Huang, W.-H.; Lee, S.-J. Anti-inflammatory effects of 7-methoxycryptopleurine and structure-activity relations of phenanthroindolizidines and phenanthroquinolizidines. *Biochem. Biophys. Res. Commun.* **2007**, *354* (4), 942–948.
- (9) NCI 60-cell assay results can be found at <http://dtp.nci.nih.gov/dtpstandard/dwindex/index.jsp>.
- (10) Gao, W.; Lam, W.; Zhong, S.; Kaczmarek, C.; Baker David, C.; Cheng, Y.-C. Novel mode of action of tylophorine analogs as antitumor compounds. *Cancer Res.* **2004**, *64* (2), 678–688.
- (11) Li, Z.; Jin, Z.; Huang, R. Isolation, total synthesis and biological activity of phenanthroindolizidine and phenanthroquinolizidine alkaloids. *Synthesis* **2001**, *16*, 2365–2378.
- (12) Chemler, S. R. Phenanthroindolizidines and phenanthroquinolizidines: promising alkaloids for anti-cancer therapy. *Curr. Bioact. Compd.* **2009**, *5* (1), 2–19.
- (13) Cusack, J. C., Jr.; Liu, R.; Baldwin, A. S., Jr. Inducible chemoresistance to 7-ethyl-10-[4-(1-piperidino)-1-piperidino]-carbonyloxy-camptothecin (CPT-11) in colorectal cancer cells and a xenograft model is overcome by inhibition of nuclear factor- κ B activation. *Cancer Res.* **2000**, *60* (9), 2323–2330.
- (14) Huang, M. T.; Grollman, A. P. Mode of action of tylocrebrine - effects on protein and nucleic-acid synthesis. *Mol. Pharmacol.* **1972**, *8* (5), 538–550.
- (15) Gupta, R. S.; Siminovitch, L. Mutants of CHO cells resistant to the protein synthesis inhibitors, cryptopleurine and tylocrebrine: genetic and biochemical evidence for common site of action of emetine, cryptopleurine, tylocrebrine, and tubulosine. *Biochemistry* **1977**, *16* (14), 3209–3214.
- (16) Gupta, R. S.; Krepinsky, J. J.; Siminovitch, L. Structural determinants responsible for the biological activity of (-)-emetine, (-)-cryptopleurine, and (-)-tylocrebrine: structure-activity relationship among related compounds. *Mol. Pharmacol.* **1980**, *18* (1), 136–143.
- (17) Dolz, H.; Vazquez, D.; Jimenez, A. Quantitation of the specific interaction of [14a-³H]cryptopleurine with 80S and 40S ribosomal species from the yeast *Saccharomyces cerevisiae*. *Biochemistry* **1982**, *21* (13), 3181–3187.
- (18) Cai, X. F.; Jin, X.; Lee, D.; Yang, Y. T.; Lee, K.; Hong, Y.-S.; Lee, J.-H.; Lee, J. J. Phenanthroquinolizidine alkaloids from the roots of *Boehmeria pinnosa* potentially inhibit hypoxia-inducible factor-1 in AGS human gastric cancer cells. *J. Nat. Prod.* **2006**, *69* (7), 1095–1097.
- (19) Rao, K. N.; Bhattacharya, R. K.; Venkatachalam, S. R. Inhibition of thymidylate synthase and cell growth by the phenanthroindolizidine alkaloids pergularinine and tylophorinidine. *Chem.-Biol. Interact.* **1997**, *106* (3), 201–212.
- (20) Rao, K. N.; Bhattacharya, R. K.; Veankatachalam, S. R. Inhibition of thymidylate synthase by pergularinine, tylophorinidine and deoxytubulosine. *Indian J. Biochem. Biophys.* **1999**, *36* (6), 442–448.
- (21) Rao, K. N.; Venkatachalam, S. R. Inhibition of dihydrofolate reductase and cell growth activity by the phenanthroindolizidine alkaloids pergularinine and tylophorinidine: the in vitro cytotoxicity of these plant alkaloids and their potential as antimicrobial and anticancer agents. *Toxicol. in Vitro* **2000**, *14* (1), 53–59.
- (22) Gao, W.; Chen, A. P.-C.; Leung, C.-H.; Gullen, E. A.; Fuerstner, A.; Shi, Q.; Wei, L.; Lee, K.-H.; Cheng, Y.-C. Structural analogs of tylophora alkaloids may not be functional analogs. *Bioorg. Med. Chem. Lett.* **2008**, *18* (2), 704–709.
- (23) Suffness, M.; Douros, J. *Anticancer Agents Based on Natural Product Models*; Academic Press: New York, 1980; pp 465–487.
- (24) Gao, W.; Bussom, S.; Grill, S. P.; Gullen, E. A.; Hu, Y.-C.; Huang, X.; Zhong, S.; Kaczmarek, C.; Gutierrez, J.; Francis, S.; Baker, D. C.; Yu, S.; Cheng, Y.-C. Structure-activity studies of phenanthroindolizidine alkaloids as potential antitumor agents. *Bioorg. Med. Chem. Lett.* **2007**, *17* (15), 4338–4342.
- (25) Wei, L.; Shi, Q.; Bastow Kenneth, F.; Brossi, A.; Morris-Natschke Susan, L.; Nakagawa-Goto, K.; Wu, T.-S.; Pan, S.-L.; Teng, C.-M.; Lee, K.-H. Antitumor agents 253. Design, synthesis, and antitumor evaluation of novel 9-substituted phenanthrene-based tylophorine derivatives as potential anticancer agents. *J. Med. Chem.* **2007**, *50* (15), 3674–3680.
- (26) Lin, J. C.; Yang, S. C.; Hong, T. M.; Yu, S. L.; Shi, Q.; Wei, L.; Chen, H. Y.; Yang, P. C.; Lee, K. H. Phenanthrene-based tylophorine-1 (PBT-1) inhibits lung cancer cell growth through the Akt and NF- κ B pathways. *J. Med. Chem.* **2009**, *52* (7), 1903–1911.
- (27) Yang, X.; Shi, Q.; Liu, Y. N.; Zhao, G.; Bastow, K. F.; Lin, J. C.; Yang, S. C.; Yang, P. C.; Lee, K. H. Antitumor agents 268. Design, synthesis, and mechanistic studies of new 9-substituted phenanthrene-based tylophorine analogues as potent cytotoxic agents. *J. Med. Chem.* **2009**, *52* (16), 5262–5268.
- (28) Wang, K.; Wang, W.; Wang, Q.; Huang, R. Efficient synthesis of aza-phenanthroindolizidine and aza-phenanthroquinolizidine and anticancer activities. *Lett. Org. Chem.* **2008**, *5* (5), 383–390.
- (29) Yang, X. M.; Shi, Q.; Bastow, K. F.; Lee, K. H. Antitumor Agents. 274. A new synthetic strategy for E-ring SAR study of antofine and cryptopleurine analogues. *Org. Lett.* **2010**, *12* (7), 1416–1419.
- (30) Alavijeh, M. S.; Chishty, M.; Qaiser, M. Z.; Palmer, A. M. Drug metabolism and pharmacokinetics, the blood-brain barrier, and central nervous system drug discovery. *NeuroRx* **2005**, *2* (4), 554–571.
- (31) Clark, D. E. In silico prediction of blood-brain barrier permeation. *Drug Discovery Today* **2003**, *8* (20), 927–933.
- (32) van de Waterbeemd, H.; Camenisch, G.; Folkers, G.; Chretien, J. R.; Raevsky, O. A. Estimation of blood-brain barrier crossing of drugs using molecular size and shape, and H-bonding descriptors. *J. Drug Target* **1998**, *6* (2), 151–165.
- (33) <http://preadmet.bmdrc.org>
- (34) Wang, Y.; Gao, W.; Svitkin, Y. V.; Chen, A. P.; Cheng, Y. C. DCB-3503, a tylophorine analog, inhibits protein synthesis through a novel mechanism. *PLoS One* **2010**, *5* (7), e11607.